Machine Learning Module for Predicting Tensile Response of SLMed Ti-6Al-4V

M. Banerjee, A. Banerjee, D. Mukherjee, A. K. Singla, and J. Singh

1 Introduction

Additive manufacturing (AM), also known as rapid prototyping (RP), is a cost-effective and time-efficient single-shot manufacturing process for intricate customized shapes (preferably low volume) produced from a digital system (3D CAD, MRI, CT scans, etc.). In particular, among the powder-based AM processes, the powder bed fusion (PBF) is categorized into two, namely selective laser melting (SLM) and selective laser sintering (SLS). During the SLM process, the powder gets completely fused in an inert environment (e.g., argon) through near-infrared wavelength laser radiation, and overlapped melt tracks get solidified to produce desired parts [1]. At present, it has appeared to be the most globally accepted approach for metal AM [2].

Among the several SLM process parameters involved in laser PBF technology, the high-power beam parameters are found to be the most effective ones for the desired output performance. The four most influencing parameters are found from

M. Banerjee (✉)
Department of Mechanical Engineering, IIT Kharagpur, Kharagpur, West Bengal, India
e-mail: mainakb_mech20@kgpian.iitkgp.ac.in

A. Banerjee
Department of Electrical Engineering, NIT Rourkela, Rourkela, Orissa, India
e-mail: ankan.banerjee95@gmail.com

D. Mukherjee
Department of Engineering, University of Cambridge, Cambridge CB2 1PZ, UK
e-mail: dm914@cam.ac.uk

A. K. Singla · J. Singh
Department of Mechanical Engineering, SLIET, Longowal, Punjab, India
e-mail: anilsingla@sliet.ac.in

J. Singh
e-mail: jagtarsingh@sliet.ac.in

N. Ramesh Babu et al. (eds.), *Advances in Additive Manufacturing and Metal Joining*,
Lecture Notes in Mechanical Engineering,
https://doi.org/10.1007/978-981-19-7612-4_18

the prolonged experimental observations to be laser power (P), scan speed (v), hatch spacing (h), and layer thickness (t) [1]. In addition, two energy densities, namely, the volumetric (E_V) and the linear energy density (E_L) are defined in terms of the four aforementioned parameters [3]

$$\mathrm{E_V}\left(\mathrm{J/mm^3}\right) = \frac{P(\mathrm{W})}{v(\mathrm{mm/sec}) \cdot h(\mu m) \cdot t(\mu m)} \tag{1}$$

$$\mathrm{E_L}(\mathrm{J/m}) = \frac{P(\mathrm{W})}{v(\mathrm{mm/sec})}, \tag{2}$$

which are observed to play a pivotal role in controlling various properties (mechanical, thermal) of the fabricated material.

Due to its high strength-to-weight ratio and good biocompatibility, titanium Ti-6Al-4V and its ELI alloys fetch most of the attention in the recent past [4]. The very requirement of the specific design of prosthetic and orthopedic parts partly necessitates the introduction of present matured three-dimensional (3D) printing technology for this titanium alloy. Moreover, for fruitful utilization of the AMed parts as structural components, namely, aircraft structures, gas turbines, biomedical implants, etc., their tensile behavior is considered to be one of the most important mechanical properties. The aforementioned behavior can be quantified via yield strength (YS), ultimate tensile strength (UTS), percentage of total elongation (TE), and elastic modulus (E). From most of the researches (~81%), it has been observed that the values of elastic modulus lie in the range of 105–120 GPa [1], which is considerably higher than the requirement for human bones (~40 GPa) [5]. Achieving the same involves mostly porous structure formation, which is not intended to include in the ongoing study.

Achieving the mechanical properties in the as-fabricated AMed components comparable to the thermo-mechanically processed ones is still found to be challenging. In fact, for the AMed parts, it has also been observed that ductility enhancement is one of the most concerns to date [6]. The reason behind this is that the components manufactured by the AM typically exhibit lesser ductility than the desired as per the ASTM standards, e.g., [2, 7].

The tensile strength is observed to depend directly on the in-process parameters involved in the AM process. For example, the consequence of increasing scan speed on decreasing tendency of all the tensile properties of Ti-6Al-4V alloy (Grade 23) samples has been reported by Gong et al. for the SLM process [8].

Machine learning (ML), on the other hand, serves as an excellent tool to predict a number of output features in modern manufacturing science, especially in 3D printing. Being a subset of artificial intelligence, it is based on rigorous algorithms through which a machine can automatically learn and improve itself from experience rather than being programmed via pre-determined models. The learning techniques are classified as supervised learning, unsupervised learning, and reinforcement learning. Supervised learning algorithms are trained using the input and the desired labeled output data. In the case of support vector machines (SVM), a

sub-category of supervised learning algorithm, respective algorithms (i.e., linear, quadratic, cubic, fine Gaussian, medium Gaussian, and coarse Gaussian) make a contrasting separation between the classes by means of corresponding nature of kernel scale.

In this context, the authors briefly mention some recent works employing ML tools to aid manufacturing and control like Ng et al. highlighted deep learning, a branch of ML, as a promising advancement in the era of 3D bio-printing emphasizing the potential of this algorithm in every phase of the printing process [9].

Khorasani et al. have studied the impact of process parameters on the relative density and involved an artificial neural network (ANN) as a part of numerical analysis [10]. For the laser melting deposition (LMD) AM process, Velázquez et al. have used a fuzzy logic-based inference system (based on the Mamdani method) for predicting the volumetric energy input on single AISI316 SS beads deposition [11].

In a different study, an ensemble learning-based algorithm was declared as well capable for surface roughness prediction in extrusion-based additive manufacturing processes, after comparing the model output with the corresponding experimental values [12]. Interestingly, another ML-based fatigue life prediction approach for AM-printed SS316L has recently been carried out by Zhan and Li training the models with continuum damage mechanics (CDM)-based experimental data involving ANN, RF, and SVM algorithms [13].

In this context, no investigation regarding the prediction of the tensile strength in terms of the AM process parameters has been reported as per the best of the authors' knowledge. Evidently, it may be acknowledged to be a very fruitful effort to expedite the tensile properties prediction involving the ML module (specifically SVM). Here, it has been further considered to carry out material-specific modeling, typically for SLM-manufactured Ti-6Al-4V alloys. As mentioned, most influencing parameters have been considered in the present study, along with two well-established energy function relationships for predicting the YS, UTS, and yielding TE of the SLM as-built samples. In the beginning, the ML module training methodology has been briefly demonstrated. During analysis, a comparison of the accuracy of ML-based classifiers has been illustrated for different combinations of training data for all the considered tensile properties each. Along with that, the variation effect of cross-validation folds has been studied on model accuracy during the classifier model training. Finally, the developed models have been probed for using the set of validation data.

2 Methodology

The tools and methods used to develop three distinct trained models for YS, UTS, and TE prediction have been discussed in the following subsections.

Table 1 Scanning parameters used for printing different SLMed Ti6A4V samples and corresponding tensile properties

P (W)	v (mm/sec)	h (μm)	T (μm)	YS (MPa)	UTS (MPa)	TE (%)	Refs.
120	960	100	30	1098	1237	8.8	[8]
120	540	100	30	1150	1257	8	[8]
120	400	100	30	1066	1148	5.4	[8]
120	1260	100	30	932	1112	6.6	[8]
120	1500	100	30	813	978	3.7	[8]
375	1029	120	60	1106	NR	11.4	[14]
194	1000	70	20	1030	NR	NR	[15]
250	1600	60	30	1125	1216	6	[16]
*170	1250	100	30	1143	1219	4.89	[17]
*275	805	120	50	1200	1280	2.4	[7]

NR = Not Reported

2.1 Database Development

The analysis for the tensile properties prediction was done on a dataset that was collected from several reputed journals and proceedings' articles, a few among these are provided in Table 1. After a rigorous data collection (number of data points for YS: 107, UTS: 95, and TE: 102) from the literature, a number of MATLAB tools and applications have been used in the present work for the predictive model preparation and testing. Here, MATLAB R2015a (8.5.0.197613) academic licensed version has been used in a 4 GB RAM and Intel CORE™ i3 supporting system capable of smoothly handling the load of the database used.

Labeling of the output data is done for all the three models based on the suitable range of values as the authors contemplate and has shown with respective results (Sects. 3.1–3.3). Instead of using the exact values, the trained models predict the range of values in terms of labels, as initially have designated before data analysis.

The authors follow the typical route to ML-based modeling and divide the latter into three categories, namely training, testing, and validation dataset. Based on the types of model validation method (cross-validation) considered, in the present case, a set of about 15% of totally collected data (e.g., marked * in Table 1) was kept separately as validation dataset for model development.

2.2 ML Model Architecture

For each of the predictive models' development, subsequent operation sequences have been followed, adhering to their respective features. After trial-and-error with

various available classifiers, a handful among them is finalized based on the trained model accuracy. As the application for the specific data-driven classification can easily be tackled in the available MATLAB versions, the authors find it redundant to show and describe the intermediate processing steps in the ongoing discussion.

In the very first stage of classification, the data matrix is imported into the classification learner application. Thereafter, the minute selection of predictor(s) and response (only one) is executed as per the users' choice. For the present work, label (L) has always been selected as a response, and for each of three matrices, all the rest variable(s) has (have) fixed as the predictor(s). At this final phase, the validation method is applied depending on its typical effectiveness based on the size of the data-set it is going to handle. In the present work, it is noticed that the dataset is sparse (~100, specific number provided in Sect. 2.1). Hence, the cross-validation method appeared to be the best one for executing the complete work.

After all the above-mentioned choices, the data is imported. Then selecting each classifier, the model is trained, and the corresponding accuracy is displayed. Finally, a comparison is made to identify the relatively accurate one based on the number of folds and classifiers of the particular choice group. In particular, the accuracy of the trained predictive model is compared among the SVM classifiers, and accordingly, the best models have been identified for respective properties. Subsequently, the model is exported for a specific model that shows the highest accuracy to test its prediction capability with already experimentally known data (test dataset).

3 Results and Discussions

After carrying out several model training with the developed data, the outcomes and consequent comprehensive observations from the three tensile behavior representing models are highlighted in the following three subsections. The authors have executed training with all the categories, but unsatisfactory accuracy made us decide not to include the irrelevant results in the present manuscript. Hence, the main focus is given to the SVM analysis in detail, and the corresponding results are graphically presented. To obtain a suitable number of folds that maximizes the model's accuracy, the fold numbers from 2 up to 32 are analyzed. For each of the typical cases, the models have been trained ten times as it is based on statistical analysis. Consequently, the mean values are carefully considered in practice and will be discussed in subsection 3.5. Trained model accuracy accordingly portrays its real-world usefulness from its applicability traits.

3.1 Yield Strength Predictive Model Training

For the GR_I category (Fig. 1e) using the YS labeled dataset (Fig. 1d), maximum predictive model accuracy is obtained to be 84.5% using the fine Gaussian SVM

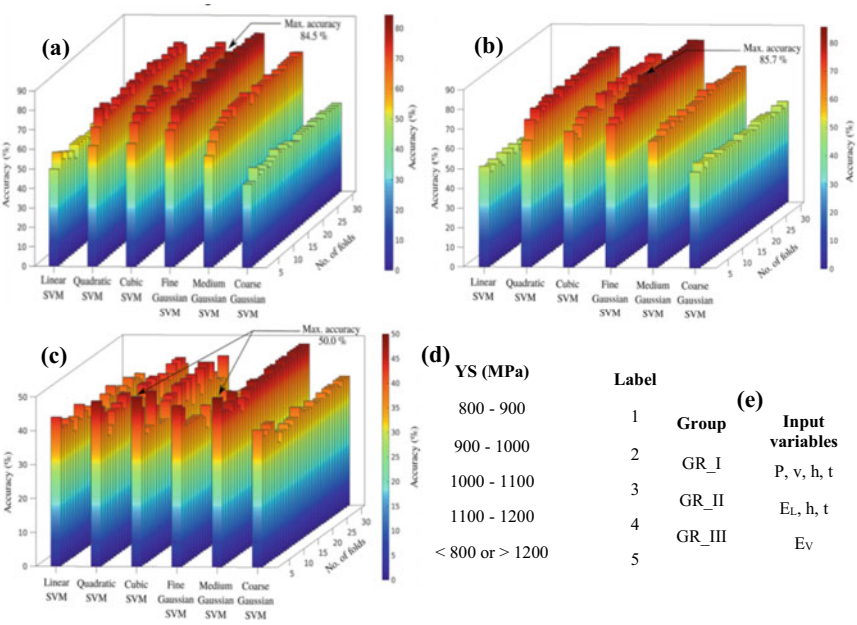

Fig. 1 3D plot for **a** GR_I, **b** GR_II and **c** GR_III YS predictive model accuracy; and **d** labeled data used during model development and **e** input variables

classifier bearing a fold number of 22 (Fig. 1a). Compared to the fine Gaussian, quadratic, and cubic, SVM classifiers show comparable model accuracy. Still, greater fluctuation in accuracy variation was observed in the latter two (~17–18%) compared to the former one (~14%); see Fig. 1a. Moreover, it is quite clear that linear and coarse Gaussian SVM is not suitable for classifying this kind of dataset. It is also observed that for smaller validation fold numbers, the trained models have shown a bit lesser accuracy compared to the higher numbers (Fig. 1a).

In the case of GR_II grouping (Fig. 1e), maximum accuracy for the trained YS predictive models is obtained for a fold number of 13 in the fine Gaussian SVM classifier as 85.7% (Fig. 1b). From the accuracy viewpoint, it has revealed an almost similar nature with the latest group of variables (GR_I). However, for the present group, the quadratic SVM classifier shows slightly better overall accuracy compared to the cubic (Fig. 1b). The changes may be interpreted as the involvement of numbers and a set of variables varied from the previous grouping (GR_I). Furthermore, throughout the change in fold numbers, quadratic shows a better fluctuation trend compared to the cubic after a few initials (Fig. 1b). The present instance also indicates the poor model behavior for training both with linear and coarse Gaussian SVM classifiers.

Finally, in the case of the GR_III combination (Fig. 1e) of the trained YS predictive model, the maximum accuracy is obtained for a fold number of 2 as 50% in both cubic and medium Gaussian SVM classifiers (Fig. 1c). In this case, an abrupt change (decrement) in the accuracy has been observed throughout, compared to the

percentage that appeared for the previous two variable groups (GR_I and GR_II). The reason behind this scenario is highly expected to be the involvement of only one labeled dataset. In this situation, overall accuracy throughout the folds was found stable in medium Gaussian SVM. Besides that, the quadratic and cubic classifiers show a similar extent of accuracy, but a fluctuation (~12–13%) is observed throughout the fold variation; see Fig. 1c.

From the three instances considered for YS model training, the overall accuracy of the model has been finally indicated as 85.7% using the GR_II variable set and fine Gaussian SVM classifier. The GR_I variable set has exhibited almost comparable utility through trained model performance. According to the validation method considered here, the model accuracy found may be deemed as moreover too satisfactory from its application viewpoint.

3.2 Ultimate Strength Predictive Model Training

In the case of GR_I combination using the UTS labeled dataset (Fig. 2d), maximum predictive accuracy is obtained as 80.4% for a fold number of 22 in the fine Gaussian SVM classifier (Fig. 2a). Moreover, it shows the accuracy of almost the same order throughout the fold variation. After fine Gaussian, the overall accuracy decreases consecutively for cubic and quadratic classifiers (Fig. 2a). Along with that, the variation in the accuracy due to cross-fold number alteration also fluctuates too much for the two aforesaid classifiers (about 28% and 21%, respectively). Notably, the linear and coarse Gaussian SVM classified the least accurate (~52%) trained models with marginally better performance (~62%) for medium Gaussian one.

For the GR_II category in the UTS predictive trained model, maximum accuracy for the model is obtained as 71.7% for the fine Gaussian SVM classifier bearing a fold number of 15 (Fig. 2b). A bit fluctuating nature has been observed throughout the fold variation for this particular case. Subsequently, models with accuracy lie in the near about ranges observed for the cubic and quadratic classifiers as depicted in the 3D plot (Fig. 2b).

Finally, the GR_III grouping for the UTS predictive model has displayed maximum accuracy for a fold number of 16 in the fine Gaussian SVM classifier as 52.2% (Fig. 2c). Also, for all the classifiers, inconsistent patterns in the model accuracy appeared as usual, like the YS model.

From the above-discussed three illustrations considered for training UTS predictive model, the overall accuracy of the model has been cumulatively indicated as 80.4% using fine Gaussian SVM classifier for GR_I variable set. From the model validation method selection aspect, the trained model's accuracy may be considered as overall satisfaction with respect to its reliable implementation viewpoint.

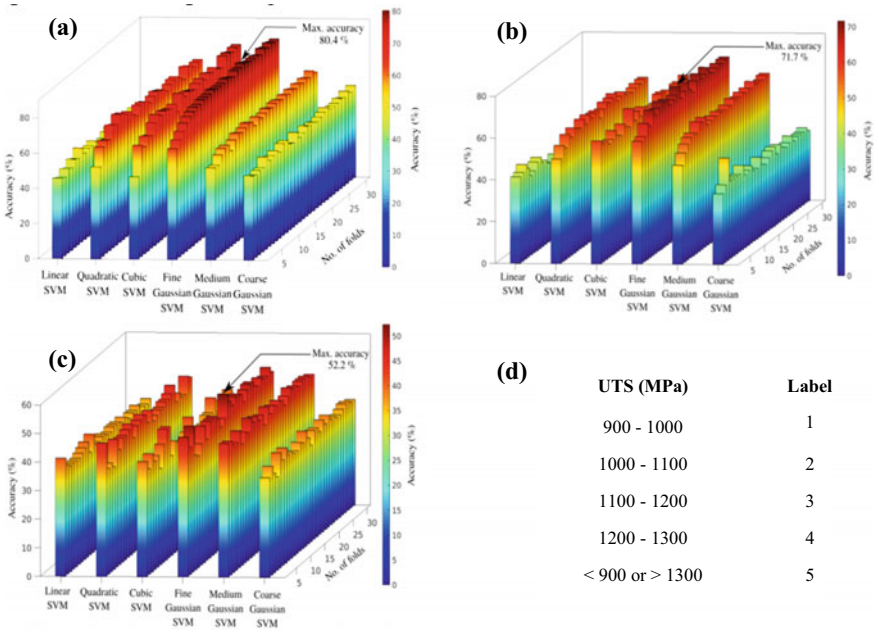

Fig. 2 3D plot for **a** GR_I, **b** GR_II and **c** GR_III UTS predictive model accuracy; and **d** labeled data used during model development

3.3 Ductility Predictive Model Training

In the case of training with the GR_I grouping using the TE labeled dataset (Fig. 3d), maximum accuracy for the predictive model is obtained for a fold number of 14 in the fine Gaussian SVM classifier as 91.7% (Fig. 3a). For a maximum of the fold variations apart from a few initials, the fluctuation in the accuracy is almost stable. After the best classifier, the overall second and third best appeared are cubic and quadratic, respectively. Linear and coarse Gaussian appeared as least effective (<50%) for the present case with a marginally better (~65%) for the medium Gaussian SVM classifier.

In the case of the GR_II variable set, the maximum accuracy for the trained model is attained for a fold number of 8 as 74% in the fine Gaussian SVM classifier (Fig. 3b). During the number of cross-fold variations, minor luctuations have been observed in the fine Gaussian except for a few initials; and it appears as prominent for the quadratic, cubic, and medium Gaussian (Fig. 3b). However, the quadratic and cubic SVM have classified the data with almost similar accuracy (~70%) comparable to the best one (fine Gaussian SVM).

Next, in the case of the GR_III category, the maximum accuracy for the model is obtained as 53.1% for the fine Gaussian SVM classifier bearing a fold number of 4 (Fig. 3c). As usual, accuracy is drastically low like the previous two modeling

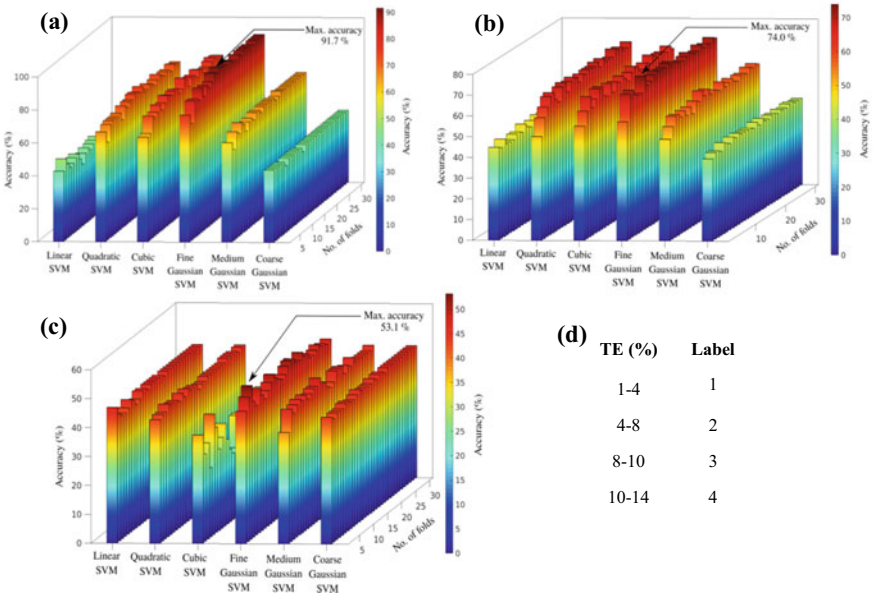

Fig. 3 3D plot for **a** GR_I, **b** GR_II, and **c** GR_III TE predictive model accuracy; and **d** labeled data used during model development

sections (Sects. 3.1 and 3.2). During the fold variations, except the cubic SVM, fine and medium Gaussian classifiers have shown comparatively remarkable fluctuations than the rest (Fig. 3c).

From the three instances discussed in the present subsection, the overall accuracy of the trained model has been finally pointed out as 91.7% using the fine Gaussian SVM classifier for the GR_I variable set. Also, it appeared to be the maximum among all the presently studied model categories. According to the currently considered validation method, the ductility predictive model accuracy, found after numerous training, may be regarded as highly satisfactory from its application perspective and expected to predict accurately in most of the future scenarios.

3.4 Validation of Trained Models

Next, the authors export the most accurate trained models for the YS, UTS, and ductility as indicated in the last three sections. For validation of each of the models, all the models of each group having the highest accuracy are now successfully authenticated with the validation dataset as already kept aside (for YS: 16, UTS: 14, and TE: 15). For a better presentation of the validation study, the results have been given in Table 2 with corresponding correctness during the trained model validation.

Table 2 Prediction correctness of trained models during validation

Variable group	YS model (%)	UTS model (%)	TE model (%)
GR_I	81.25	85.71	93.33
GR_II	87.50	71.43	80
GR_III	62.5	57.14	46.67

3.5 Discussions

From the whole model training outcomes, it can be inferred that it is hardly possible to achieve too much accurate predictive model through ML for such a specific model condition considered in the current work. There may exist plenty of reasons for this deviation of the trained model's output from real-life experimentation. According to the trailing discussion, four variables have been considered, in individual or the form of already traditional relations. Evidently, the rest of the huge printing parameter-family may act as a noise factor in different extents as per situations. Few of the relevant instances have been mentioned in the subsequent discussions, primarily focusing on the tensile properties considering specific material (Ti-6Al-4V) and printing process (SLM).

It has been highlighted by Agius et al. in their review work that the properties are affected due to different laser scanning strategies [18]. Pal et al. observed the significant effect of different building orientations on the tensile properties through building samples in four different directions [19]. As a consequence of minimizing the aforementioned influence, all the data considered for the current study are typically for vertically built (along z-direction) samples.

Furthermore, the influence of the variation of focal offset distance [3], inter-layer time [3, 20], and powder bed temperature [3, 21] has appeared as effective on the tensile properties of SLM as-built Ti-6Al-4V samples. From the broad observations, it may be said that different printing systems usually affect the mechanical properties to some extent.

Despite all the concerns regarding deviation in predictions, accuracy in all the three subdivisions was found well satisfactory (>80%) from an implementation viewpoint. Most interestingly, as a most concerned property among the SLM as-built structures, the ductile behavior predictive model achieved the highest (>90%) accuracy. As indicated at the very beginning of the current section regarding obvious consideration of the mean values, a glimpse of observed deviations in the accuracy has been marked in the bar chart (Fig. 4) just for providing the impression cumulatively.

4 Conclusions and Future Perspectives

Based on the behavior of trained models' accuracy, the following brief remarks may be provided in terms of its operative and consistent solicitation:

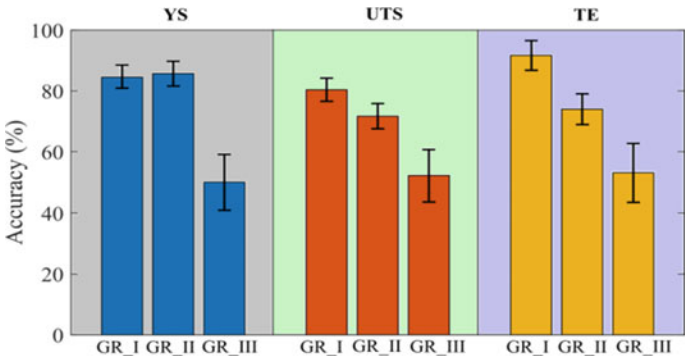

Fig. 4 Accuracy variations during model training

- Based on the tendency of the input dataset, the fruitful functionality of the classifier changes in terms of the model accuracy. For any particular classifier, a too abrupt shift in model accuracy has not been observed for all the instances, as desired. However, minor changes were found due to variations in the number of folds.
- The accuracy of the GR_III variable set is too low (~50%) on average in comparison with the other two groups (GR_I and GR_II). Hence, the GR_III group may be discarded any further to train the ML module for the AMed parts.
- For model development involving 3D printing parameters, the fine Gaussian SVM classifier is found to be most useful as a whole from the present training–testing trend through the ML algorithm. For YS, UTS, and TE predictive models, the maximum accuracy of the models is obtained as 85.7%, 80.4%, and 91.7%, respectively, using the fine Gaussian SVM classifier.

To gain further acceptance from the industry as well as in research and development, separate model development using ML modules can be expedited in AM for other mechanical properties like fatigue strength, tribological behavior, microhardness, impact strength, etc. ML algorithms also can be utilized to predict the properties of thermally and mechanically post-treated components at specified conditions. The authors expect that the present work would surely provide an adequate paradigm to future researchers in the advancement of time and cost-effective AM process.

References

1. AK Singla M Banerjee A Sharma J Singh A Bansal MK Gupta N Khanna AS Shahi DK Goyal 2021 Selective laser melting of Ti6Al4V alloy: process parameters, defects and post-treatments J. Manuf. Process 64 161 187
2. WSW Harun MSIN Kamariah N Muhamad SAC Ghani F Ahmad Z Mohamed 2018 A review of powder additive manufacturing processes for metallic biomaterials Powder Technol. 327 128 151

3. H Shipley D McDonnell M Culleton R Coull R Lupoi G O'Donnell D Trimble 2018 Optimisation of process parameters to address fundamental challenges during selective laser melting of Ti-6Al-4V: a review Int. J. Mach. Tools Manuf. 128 1 20
4. H Eskandari Sabzi 2019 Powder bed fusion additive layer manufacturing of titanium alloys Mater. Sci. Technol. (United Kingdom) 35 875 890
5. F Trevisan F Calignano A Aversa G Marchese M Lombardi S Biamino D Ugues D Manfredi 2018 Additive manufacturing of titanium alloys in the biomedical field: processes, properties and applications J. Appl. Biomater. Funct. Mater. 16 57 67
6. D Herzog V Seyda E Wycisk C Emmelmann 2016 Additive manufacturing of metals Acta. Mater. 117 371 392
7. A Popovich V Sufiiarov E Borisov I Polozov 2015 Microstructure and mechanical properties of Ti-6AL-4V manufactured by SLM Key Eng. Mater. 651–653 677 682
8. H Gong K Rafi H Gu GD Janaki Ram T Starr B Stucker 2015 Influence of defects on mechanical properties of Ti-6Al-4V components produced by selective laser melting and electron beam melting Mater. Des. 86 545 554
9. WL Ng A Chan YS Ong CK Chua 2020 Deep learning for fabrication and maturation of 3D bioprinted tissues and organs Virtual Phys. Prototyp. 15 340 358
10. AM Khorasani I Gibson AH Ghasemi A Ghaderi 2019 A comprehensive study on variability of relative density in selective laser melting of Ti-6Al-4V Virtual Phys. Prototyp. 14 349 359
11. Tasé Velázquez, D.R., Helleno, A.L., de Oliveira, M.C., Fals, H.C., Macias, E.J.: Fuzzy logic-based inference system for prediction of energy input in laser metal deposited Aisi316 single-beads. In: 32nd European modelling simulation symposium EMSS 2020. pp. 400–409. (2020)
12. Z Li Z Zhang J Shi D Wu 2019 Prediction of surface roughness in extrusion-based additive manufacturing with machine learning Robot. Comput. Integr. Manuf. 57 488 495
13. Zhan, Z., Li, H.: Machine learning based fatigue life prediction with effects of additive manufacturing process parameters for printed SS 316L. Int. J. Fatigue. **142**, 105941 (2021)
14. W Xu M Brandt S Sun J Elambasseril Q Liu K Latham K Xia M Qian 2015 Additive manufacturing of strong and ductile Ti-6Al-4V by selective laser melting via in situ martensite decomposition Acta Mater. 85 74 84
15. J Han J Yang H Yu J Yin M Gao Z Wang X Zeng 2017 Microstructure and mechanical property of selective laser melted Ti6Al4V dependence on laser energy density Rapid Prototyp. J. 23 217 226
16. V Cain L Thijs J Humbeeck Van B Hooreweder Van R Knutsen 2015 Crack propagation and fracture toughness of Ti6Al4V alloy produced by selective laser melting Addit. Manuf. 5 68 76
17. HK Rafi TL Starr BE Stucker 2013 A comparison of the tensile, fatigue, and fracture behavior of Ti-6Al-4V and 15–5 PH stainless steel parts made by selective laser melting Int. J. Adv. Manuf. Technol. 69 1299 1309
18. Agius D, Kourousis KI, Wallbrink C (2018) A review of the as-built SLM Ti-6Al-4V mechanical properties towards achieving fatigue resistant designs. Metals 8(1):75
19. Pal S, Gubeljak N, Hudak R, Lojen G, Rajtukova V, Predan J, Kokol V, Drstvensek I (2019). Tensile properties of selective laser melting products affected by building orientation and energy density. Mater Sci Eng A 743:637–647
20. Xu W, Lui EW, Pateras A, Qian M, Brandt MJ (2017) In situ tailoring microstructure in additively manufactured Ti-6Al-4V for superior mechanical performance. Acta Materialia 125:390–400
21. Ali H, Ma L, Ghadbeigi H, Mumtaz K (2017) In-situ residual stress reduction, martensitic decomposition and mechanical properties enhancement through high temperature powder bed pre-heating of Selective Laser Melted Ti6Al4V. Mater Sci Eng A 695:211–220